

# Lattice Boltzmann equation method in electrohydrodynamic problems

A.L. Kupershtokh<sup>a,\*</sup>, D.A. Medvedev<sup>a,b</sup>

<sup>a</sup>*Laurentyev Institute of Hydrodynamics of Siberian Branch of Russian Academy of Sciences, Novosibirsk 630090, Russia*

<sup>b</sup>*Otto-von-Guericke University Magdeburg, Magdeburg, Germany*

Available online 8 November 2005

## Abstract

A consistent lattice Boltzmann equation (LBE) model for simulating different electrohydrodynamic (EHD) phenomena is developed. The model includes fluid dynamics, electric charge transport via advection and conduction currents, and action of electric forces upon space charges in liquid. Problems with different thermodynamic phases (liquid and gaseous) and phase transitions, and with inhomogeneous and density-dependent electric permittivity and conductivity can also be simulated, as well as charge injection and recombination. Deformations and breakup of conductive vapor bubbles, bubble deformation due to electrostriction, dynamics of drops with different electric permittivity were simulated. Simulations show the great potential of the method especially for problems with free boundaries (systems with vapor bubbles and multiple components with different electric properties).

© 2005 Elsevier B.V. All rights reserved.

*Keywords:* Electrohydrodynamics; Lattice Boltzmann equation; Bubbles; Electrostriction

## 1. Introduction

In simulations of electrohydrodynamic (EHD) problems, following physical phenomena should be consistently modeled: hydrodynamics, transport of electric charge carriers, evolution of electric potential distribution, action of electric field on charged liquid.

The lattice Boltzmann equation (LBE) methods [1–3] are widely used for solving the hydrodynamic Navier–Stokes equations. Because of their kinetic nature, these methods possess high numerical stability, and complex boundary conditions are easy to implement. Multiphase and multi-component flows can also be simulated with moderate computation cost.

Finite-difference methods were previously used for calculation of charge transfer. In these methods, the value of charge diffusivity is large enough [4,5]. Moreover, it is not constant and depends on velocity of fluid  $\mathbf{u}$  as  $D = \Delta t |\mathbf{u}| (h/\Delta t - |\mathbf{u}|)/2$  [5]. In [5], we proposed another method to calculate convective and diffusive charge transport in that charge diffusivity is velocity-independent and can be adjusted.

In present work, we used the LBE methods for solving the equations for concentrations of electric charge carriers.

## 2. Equations

Hydrodynamic equations are the continuity equation

$$\frac{\partial \rho}{\partial t} + \text{div}(\rho \mathbf{u}) = 0 \quad (1)$$

and the Navier–Stokes equation

$$\frac{\partial \rho \mathbf{u}}{\partial t} + \nabla \Pi_{\alpha\beta}^{(0)} = \mathbf{F} + \eta \nabla^2 \mathbf{u} + \left( \zeta + \frac{\eta}{3} \right) \text{grad div } \mathbf{u}. \quad (2)$$

Here,  $\rho$  is the density of liquid,  $\mathbf{u}$  is the velocity of fluid flow,  $\Pi_{\alpha\beta}^{(0)} = p\delta_{\alpha\beta} + \rho u_\alpha u_\beta$  is the non-viscous part of the momentum flux tensor.

Equations for concentrations  $n_i$  of carriers of electric charge are

$$\frac{\partial n_i}{\partial t} + \text{div}(n_i \mathbf{u}) = D_i \nabla^2 n_i - \text{div} \left( \frac{q_i}{|q_i|} b_i n_i \mathbf{E} \right) + w_i - r_i. \quad (3)$$

Here,  $D_i$  are the diffusivities,  $b_i$  are the macroscopic effective mobilities of charges carriers  $q_i$ ;  $w_i$ ,  $r_i$  are the rates of ionization and recombination of charge carriers.

\*Corresponding author.

*E-mail addresses:* [skn@hydro.nsc.ru](mailto:skn@hydro.nsc.ru), [skn@demakova.net](mailto:skn@demakova.net)  
(A.L. Kupershtokh).

The Poisson's equation for potential of electric field  $\varphi$  is

$$\operatorname{div}(\varepsilon \nabla \varphi) = -4\pi q, \quad \mathbf{E} = -\nabla \varphi. \quad (4)$$

The electric force acting on a liquid with the space charge  $q = \sum q_i n_i$  in an electric field is

$$\mathbf{F} = q\mathbf{E} - \frac{E^2}{8\pi} \nabla \varepsilon + \frac{1}{8\pi} \nabla \left( E^2 \rho \frac{\partial \varepsilon}{\partial \rho} \right). \quad (5)$$

The electric current can be expressed as

$$\mathbf{j} = \sum (q_i n_i \mathbf{u} - D_i q_i \nabla n_i + b_i |q_i| n_i \mathbf{E}) = q\mathbf{u} - \sum D_i q_i \nabla n_i + \sigma \mathbf{E}. \quad (6)$$

Here, the local conductivity  $\sigma = \sum b_i |q_i| n_i$  depends on local concentrations of charge carriers and can vary in space and in time.

### 3. Method of splitting

To solve the system of Eqs. (1)–(5), the method of splitting in physical processes [6] is used. The whole time step is divided into several stages implemented sequentially. These stages are:

1. Modeling of hydrodynamic flows.
2. Simulation of convective transport and diffusion of charge carriers.
3. Calculation of electric potential and charge transfer due to mobility of charge carriers.
4. Calculation of electrostatic forces acting on space charges in liquid.
5. Simulation of phase transition or interaction between immiscible liquids.

#### 3.1. Modeling of hydrodynamic flows

For simulation of hydrodynamic flows, the LBE method [1–3] was used. The evolution equations for single-particle distribution functions  $N_k(\mathbf{x}, t)$  have the form

$$N_k(\mathbf{x} + \mathbf{c}_k \Delta t, t + \Delta t) = N_k(\mathbf{x}, t) + (N_k^{\text{eq}}(\rho, \mathbf{u}(\mathbf{x}, t)) - N_k(\mathbf{x}, t)) / \tau + \Delta N_k, \quad (7)$$

where  $\mathbf{c}_k$  are the particle velocities,  $\Delta t$  is the time step (lattice vectors are  $\mathbf{e}_k = \mathbf{c}_k \Delta t$ ),  $\Delta N_k$  are the changes of distribution functions due to action of volume forces.

Equilibrium distribution functions are

$$N_k^{\text{eq}}(\rho, \mathbf{u}) = \rho w_k \left( 1 + 3\mathbf{c}_k \mathbf{u} + \frac{9(\mathbf{c}_k \mathbf{u})^2}{2} - \frac{3\mathbf{u}^2}{2} \right). \quad (8)$$

Here,  $\rho = \sum_k N_k$  and  $\rho \mathbf{u} = \sum_k \mathbf{c}_k N_k$ . For the two-dimensional nine-velocity D2Q9 model [3] ( $|\mathbf{c}_k| = 0, 1$  or  $\sqrt{2}$ ) on a square lattice (Fig. 1), the weight coefficients are  $w_0 = 4/9$ ,  $w_{1-4} = 1/9$ , and  $w_{5-8} = 1/36$ . The reduced relaxation time  $\tau$  determines the kinematic viscosity  $\nu = (h^2/3\Delta t)(\tau - 1/2)$ .

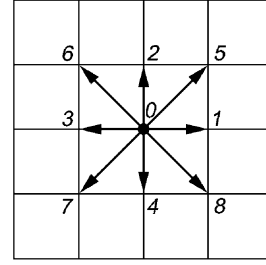


Fig. 1. Set of particle velocities  $\mathbf{c}_k$  for LBE model D2Q9.

The exact difference method (EDM) was specially developed for LBE [7,8] to take into account the action of electric forces on space charges in a liquid

$$\Delta N_k = N_k^{\text{eq}}(\rho, \mathbf{u} + \Delta \mathbf{u}) - N_k^{\text{eq}}(\rho, \mathbf{u}). \quad (9)$$

Here  $\Delta \mathbf{u} = \mathbf{F} / \rho \cdot \Delta t$  is the velocity change due to body force  $\mathbf{F}$  during time step  $\Delta t$ .

#### 3.2. Convective transport and diffusion of charge carriers

Equations of convective transport of every type of charge carriers and their diffusion, ionization and recombination

$$\frac{\partial n_i}{\partial t} + \operatorname{div}(n_i \mathbf{u}) = D_i \nabla^2 n_i + w_i - r_i \quad (10)$$

are solved using the method of additional LBE components with zero mass (passive scalar) [5] similar to one used in [9].

The evolution equations for distribution functions  $Q_{ki}(\mathbf{x}, t)$  for every type of charge carriers  $q_i$  are

$$Q_{ki}(\mathbf{x} + \mathbf{c}_k \Delta t, t + \Delta t) = Q_{ki}(\mathbf{x}, t) - (Q_{ki}(\mathbf{x}, t) - Q_{ki}^{\text{eq}}) / \tau_i. \quad (11)$$

Equilibrium distribution functions  $Q_{ki}^{\text{eq}}(n_i, \mathbf{u})$  depend on concentrations of corresponding type of charge carriers  $n_i = \sum_k Q_{ki}$  and on fluid velocity  $\mathbf{u}$ :

$$Q_{ki}^{\text{eq}}(n_i, \mathbf{u}) = n_i w_k \left( 1 + 3\mathbf{c}_k \mathbf{u} + \frac{9(\mathbf{c}_k \mathbf{u})^2}{2} - \frac{3\mathbf{u}^2}{2} \right). \quad (12)$$

Diffusivities  $D_i = (h^2/3\Delta t)(\tau_i - 1/2)$  can be adjusted independently changing the relaxation times  $\tau_i$ .

The exact values of rates of ionization  $w_i$  and recombination  $r_i$  of charge carriers in liquids are unknown, but some discussion and approximate laws for weakly conductive liquids could be found in [10].

#### 3.3. Calculation of electric potential and charge transport due to mobility of charge carriers (conductivity)

Transport of electric charge via mobility of charges carriers in electric field is computed simultaneously with the solution of the Poisson equation for potential of electric field. The time-implicit finite-difference equations for charge transport equations and for Poisson equation were solved by the method of iterations relatively values of all

concentrations of charge carriers  $n_i^{n+1}$  and values of potential  $\varphi^{n+1}$  at the next time step at every node

$$n_i^{n+1} = n_i^n + \Delta t \operatorname{div} \left( \frac{q_i}{|q_i|} b_i n_i^{n+1} \nabla \varphi^{n+1} \right),$$

$$\operatorname{div}(\varepsilon \nabla \varphi^{n+1}) = -4\pi \sum q_i n_i^{n+1}. \quad (13)$$

In the simplest case of constant and equal coefficients  $D_i = D$ , only one equation for total charge density

$$\partial q / \partial t + \operatorname{div}(\mathbf{q}\mathbf{u}) = D \nabla^2 q - \operatorname{div}(\sigma \mathbf{E}) \quad (14)$$

can be considered instead of the set of Eq. (3). In this case time-implicit finite-difference equation for the total charge density  $q$  can be substituted directly into the finite-difference Poisson equation as in [11].

### 3.4. Action of electrostatic forces on space charges in liquid

We used a usual formula (5) for the force acting on a liquid in an electric field. Components of the electric force were calculated with a finite-difference method. Then the EDM method (9) was applied to calculate new distribution functions.

### 3.5. Phase transitions

Phase transitions are simulated in LBE method using the method of Shan and Chen [12,13]. To describe the phase transition in this model, the attractive forces were introduced between every pair of neighbor nodes. For two-dimensional case we have

$$\mathbf{F}(\mathbf{x}) = \psi(\rho(\mathbf{x})) \sum_k G_k \psi(\rho(\mathbf{x} + \mathbf{e}_k)) \mathbf{e}_k. \quad (15)$$

Here  $G_k > 0$  are the coefficients that are different for basic and diagonal directions,  $\psi(\rho)$  is an increasing function of density (effective mass). We used the following function suggested in [12]

$$\psi(\rho) = \rho_0 (1 - \exp(-\rho/\rho_0)). \quad (16)$$

To ensure the isotropy of space, coefficients for the force must satisfy the equation  $G_1 = G_0/4$ . Here,  $G_0$  is the coefficient for basic directions, and  $G_1$  is the coefficient for diagonal directions. In this case, the equation of state for isothermal model is

$$P = \rho \theta - \frac{3}{2} G_0 \psi^2(\rho), \quad (17)$$

where  $\theta = kT/m$  is the reduced temperature. In the series of isothermal LBE models: one-dimensional model D1Q3, two-dimensional model D2Q9 and three-dimensional model D3Q19, the appropriate reduced temperature is  $\theta = (h/\Delta t)^2/3$ . The critical point is  $G_{0*} = 4\theta/(3\rho_0)$  and  $\rho_* = \rho_0 \ln 2$ . For the values of  $G_0 > G_{0*}$ , coexistence of dense (liquid) and rarefied (gaseous) phases is possible.

In this case interfaces between liquid and gas are represented as thin transition layers of finite width (several nodes of lattice) where density changes smoothly from one

bulk value to another. The forces (15) ensure the surface tension of liquid–gas interface. The value of surface tension  $\lambda$  depends on value of parameter  $G_0$  [13]. The value of surface tension was measured from two-dimensional computer simulations of steady-state circular drops of different radius  $R$ . The pressure difference inside and outside a bubble was plotted as a function of the inverse radius of bubble (Laplace's law:  $P_{\text{in}} - P_{\text{out}} = \lambda/R$ ). As value of  $G_0$  approaches the critical value, the distinction between the two phases becomes negligible as it should be. For  $G_0 = 0.5$ , the surface tension is  $\lambda = 0.019$  in dimensionless units ( $\rho_0 = 1$ ,  $\tau = 1$ ).

### 3.6. Simulation of immiscible liquids

For simulations with two immiscible liquids, we used the method of Shan and Chen [12]. In the simplest case, the interactions between every neighbor nodes were introduced in form

$$\mathbf{F}_s(\mathbf{x}) = \psi(\rho_s(\mathbf{x})) \sum_{\lambda} \sum_k G_{ks\lambda} \psi(\rho_{\lambda}(\mathbf{x} + \mathbf{e}_k)) \mathbf{e}_k. \quad (18)$$

Here, we denote the components by the indexes  $s$  and  $\lambda$ . In the case of two liquids, every index can take values 1 or 2.  $\rho_s$  are the densities of components at the nodes.

The total fluid density at a node depends on densities of components as  $\rho = \sum_s \rho_s$ , where  $\rho_s = \sum_{ks} N_{ks}$ . Here,  $N_{ks}$  are the single-particle distribution functions for each component. The total momentum at a node is  $\rho \mathbf{u} = \sum_s \rho_s \mathbf{u}_s$ , where  $\mathbf{u}$  is the mean velocity,  $\rho_s \mathbf{u}_s = \sum_{ks} N_{ks} \mathbf{c}_k$  are the momenta of components. The interaction forces change the velocity of each component at the node  $\Delta \mathbf{u}_s = \mathbf{F}_s \Delta t / \rho_s$ , that should be taken into account in the collision operator for every component  $\Omega_{ks}(\rho_s, \mathbf{u}_s)$ . In our simulations, we used the same relaxation time  $\tau$  for different liquids. It means that the viscosities of these liquids were equal.

In simulations with two immiscible liquids without phase transition, we used  $G_{kss} = 0$ ,  $G_{ks\lambda} = G_{k\lambda s} > 0$ ,  $G_{1s\lambda} = G_{0s\lambda}/4$  and the following simplest function  $\psi(\rho) = \rho$ .

## 4. Results

We investigated deformation and fragmentation of conductive gas bubbles in electric field, the dynamics of gas bubbles caused by electrostriction, and deformation of liquid drops with electric permittivity different from this of main liquid. Since our simulations are mainly qualitative, we do not think that the introduction of dimensional units would be reasonable at this stage of investigation. Hence, we used the arbitrary (dimensionless) units for all parameters and variables (time, space, density, conductivity, surface tension, electric field, etc.).

The electric strength of gases is much lower than that of liquids. Hence, the electric breakdown occurs when vapor bubbles grow to a certain critical size. After breakdown, the bubble becomes conductive, and it is deformed under the action of electric field. The dynamics of bubble

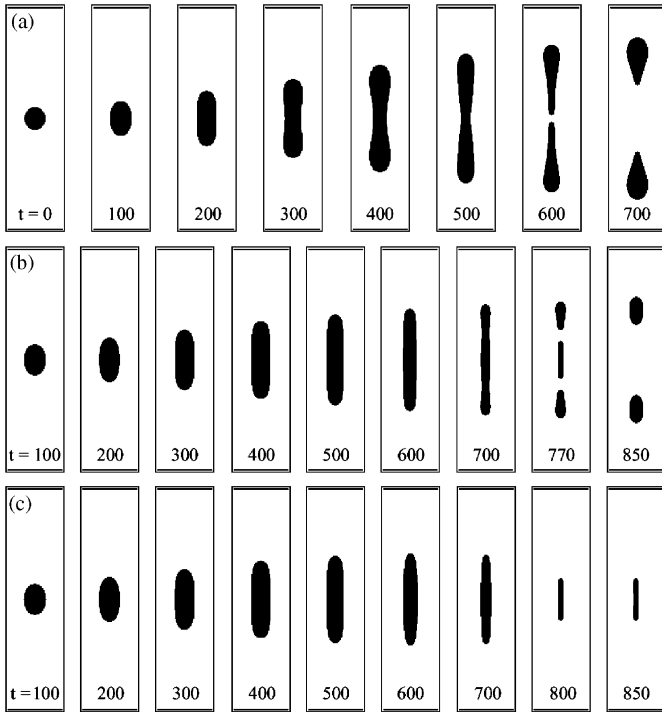


Fig. 2. Deformation and breakup of vapor bubble in electric field at different conductivity inside the bubble: (a)  $\sigma = 0.5$ ; (b)  $\sigma = 0.375$ ; (c)  $\sigma = 0.2$ . Lattice size  $250 \times 65$ .

deformation is shown in Fig. 2. Dark color corresponds to lower density.

At comparatively high conductivity, bubble grows and elongates (see Fig. 2a). Then, a neck arises at the equator, and bubble breaks into two smaller ones.

At lower conductivity inside the bubble, the deformation proceeds slower, and two necks can appear resulting in the emission of two bubbles from the poles of the original one (Fig. 2b). The central bubble has practically no charge and, hence, it collapses rapidly.

Finally, in the case of even lower conductivity, the external pressure prevails, and the bubble first elongates and then collapses (Fig. 2c).

Similar processes are observed at the breakdown of dielectric liquids [14]. At the incomplete breakdown, the streamer channel decays to the chain of bubbles that then disappear rapidly.

Usually, electric permittivity of substances depends on density. This leads to deformation of samples in electric field (electrostriction). We simulated the evolution of a bubble in dielectric liquid with permittivity  $\varepsilon = 1 + \rho/\rho_e$ . In this case,  $\rho(\partial\varepsilon/\partial\rho) = \varepsilon - 1$ , and formula (5) can be rewritten as  $\mathbf{F} = ((\varepsilon - 1)/8\pi)\nabla E^2$  (free charge density is zero).

Results are shown in Fig. 3. Dark color corresponds to lower density. Electrodes were placed at the top and bottom boundaries of computation area. The periodic boundary conditions are used at the side boundaries. When the voltage was applied, the bubble gradually elongated and later broke into two smaller ones, similar to the case of

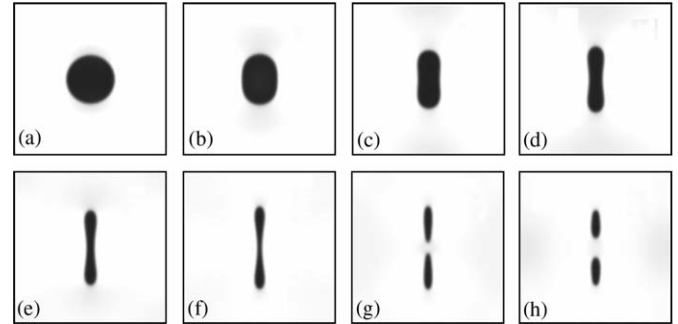


Fig. 3. Deformation of vapor bubble due to electrostriction. Average electric field  $E_a = 1.2$ .  $t = 60$  (a), 180 (b), 300 (c), 400 (d), 500 (e), 600 (f), 700 (g), 800 (h).

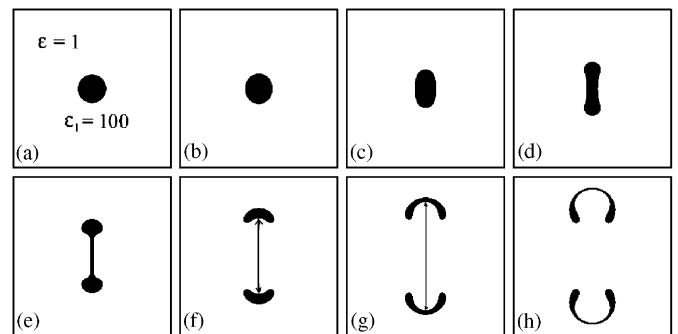


Fig. 4. Liquid drop with electric permittivity different from one of main liquid dielectric in external electric field.  $\varepsilon_1 = 100$ ,  $E_a = 0.035$ .  $t = 0$  (a), 100 (b), 200 (c), 300 (d), 400 (e), 500 (f), 600 (g), 700 (h).

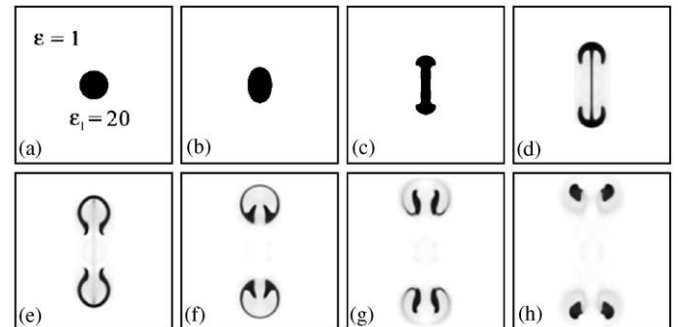


Fig. 5. Liquid drop with electric permittivity different from one of main liquid dielectric in external electric field.  $\varepsilon_1 = 20$ ,  $E_a = 0.1$ .  $t = 0$  (a), 100 (b), 200 (c), 300 (d), 400 (e), 500 (f), 600 (g), 700 (h).

conductive bubble (Fig. 2a). The total volume of the bubble also decreased due to the compression by electrostriction forces.

Elongation of bubble decreases with decrease of average electric field, and there is a threshold field magnitude below which the disruption of a bubble does not occur, that is in qualitative agreement with results of [15,16].

The dynamics of liquid drops with electric permittivity  $\varepsilon_1$  different from permittivity of main dielectric liquid ( $\varepsilon = 1$ ) in external electric field was studied (Figs. 4 and 5).

In the case shown in Fig. 5, the vortices are more pronounced than for simulation shown in Fig. 4 despite the

lower value of  $\varepsilon_1$ . The reason of this is the higher value of external electric field  $E_a$  resulting in higher electric forces that are proportional to  $\varepsilon E_a^2(\varepsilon_1 - \varepsilon)/\varepsilon_1$ .

## 5. Discussion and conclusions

A new method for simulating the EHD phenomena is developed. It provides the consistent model of all physical processes involved. Hydrodynamic flows and convective and diffusive transport of charge carriers are simulated by the LBE scheme, as well as interaction of liquid components and phase transitions and action of electric forces on a charged liquid. Evolution of potential distribution and conductive charge transport are calculated using the finite difference method.

Simulations show the great potential of the method especially for problems with free boundaries (systems with vapor bubbles and multiple components with different electric properties).

## Acknowledgments

This work was supported by the Russian Foundation for Basic Research (Grant No. 03-02-16474).

## References

- [1] G.R. McNamara, G. Zanetti, Use of the Boltzmann equation to simulate lattice-gas automata, *Phys. Rev. Lett.* 61 (1988) 2332.
- [2] F.J. Higuera, J. Jimenez, Boltzmann approach to lattice gas simulations, *Europhys. Lett.* 9 (1989) 663.
- [3] Y.H. Qian, D. d’Humières, P. Lallemand, Lattice BGK models for Navier–Stokes equation, *Europhys. Lett.* 17 (1992) 479.
- [4] D.A. Medvedev, A.L. Kupershtokh, Use of the lattice Boltzmann equation method to simulate charge transfer and electrohydrodynamic phenomena in dielectric liquids, *Proceedings of the Second International Workshop on Electrical Conduction, Convection, and Breakdown in Fluids*, Grenoble, France, 2000, pp. 60–63.
- [5] D.A. Medvedev, A.L. Kupershtokh, Modeling of electrohydrodynamic flows and micro-bubbles generation in dielectric liquid by lattice Boltzmann equation method, *Proceedings of the 14th International Conference on Dielectric Liquids*, IEEE No. 02CH37319, Graz, Austria, 2002, pp. 45–48.
- [6] N.N. Yanenko, *The Method of Fractional Steps*, Springer, Berlin, 1967.
- [7] A.L. Kupershtokh, Calculations of the action of electric forces in the lattice Boltzmann equation method using the difference of equilibrium distribution functions, *Proceedings of the Seventh International Conference on Modern Problems of Electrophysics and Electrohydrodynamics of Liquids*, St. Petersburg University, St. Petersburg, Russia, 2003, pp. 152–155.
- [8] A.L. Kupershtokh, Incorporating a body force term into the lattice Boltzmann equation, *Bulletin of Novosibirsk State University: Series of Mathematics, Mechanics and Informatics*, vol. 4(2), 2004, p. 75 (in Russian).
- [9] X. Shan, Simulation of Rayleigh–Bénard convection using a lattice Boltzmann method, *Phys. Rev. E* 55 (1997) 2780.
- [10] M.S. Apfelbaum, The prebreakdown EHD equations for liquid insulators, *Proceedings of the Seventh International Conference on Modern Problems of Electrophysics and Electrohydrodynamics of Liquids*, St. Petersburg University, St. Petersburg, Russia, 2003, pp. 9–13.
- [11] D.I. Karpov, A.L. Kupershtokh, Models of streamers growth with “physical” time and fractal characteristics of streamer structures, *Conference Record of the 1998 IEEE International Symposium on Electrical Insulation*, IEEE No. 98CH36239, Arlington, USA, 1998, pp. 607–610.
- [12] X. Shan, H. Chen, Lattice Boltzmann model for simulating flows with multiple phases and components, *Phys. Rev. E* 47 (1993) 1815.
- [13] X. Shan, H. Chen, Simulation of nonideal gases and liquid–gas phase transitions by the lattice Boltzmann equation, *Phys. Rev. E* 49 (1994) 2941.
- [14] L. Costeanu, O. Lesaint, On mechanisms involved in the propagation of subsonic positive streamers in cyclohexane, *Proceedings of the 14th International Conference on Dielectric Liquids*, IEEE No. 02CH37319, Graz, Austria, 2002, pp. 143–146.
- [15] C.G. Garton, Z. Krasucki, Bubble in insulating liquids: stability in an electric field, *Proc. R. Soc. A* 280 (1964) 211.
- [16] S. Ogata, K. Tan, K. Nishijima, J.-S. Chang, Development of improved bubble disruption and dispersion technique by an applied electric field method, *AIChE J.* 31 (1985) 62.